ARTICLE IN PRESS
+ MODEL
Frontiers of Architectural Research xxx (xxxx) xxx

Higher Education Press

Available online at www.sciencedirect.com
ScienceDirect
journal homepage: www.keaipublishing.com/foar

SOUTHEAST UNIVERSITY

RESEARCH ARTICLE

Solar radiation-based method for early design stages to balance daylight and thermal comfort in office buildings

Abel Sepúlveda [a,b,*], Seyed Shahabaldin Seyed Salehi [a], Francesco De Luca [a], Martin Thalfeldt [a,c]

[a] *Department of Civil Engineering and Architecture, Tallinn University of Technology, Tallinn 19086, Estonia*
[b] *Institute of Design and Civil Engineering, Karlsruhe Institute of Technology, Karlsruhe 76131, Germany*
[c] *FinEst Centre for Smart Cities (FinEst Centre), Tallinn University of Technology, Tallinn 19086, Estonia*

Received 5 May 2023; received in revised form 29 June 2023; accepted 5 July 2023

KEYWORDS
Cooling sizing;
Cold climate;
Solar access;
Daylight;
View out;
Window sizing

Abstract There is a lack of facade design methods for early design stages to balance thermal comfort and daylight provision that consider the obstruction angle as an independent variable without using modeling and simulations. This paper aims to develop easy-to use solar radiation-based prediction method for the design of office building facades (i.e., design parameters: room size, window-to-floor ratio, and glazing thermal/optical properties) located in urban canyons to balance daylight provision according to the European standard EN 17037:2018 and thermal comfort through specific cooling capacity. We used a simulation-based methodology that includes correlation analyses between building performance metrics and design parameters, the development of design workflows, accuracy analysis, and validation through the application of the workflows to a new development office building facades located in Tallinn, Estonia. The validation showed that the mean percentage of right/conservative predictions of thermal comfort classes is 98.8% whereas for daylight provision, it is higher than 75.6%. The use of the proposed prediction method can help designers to work more efficiently during early design stages and to obtain optimal performative solutions in much shorter time: window sizing in 73,152 room combinations in 80 s.

* Corresponding author.
E-mail address: absepu@taltech.ee (A. Sepúlveda).
Peer review under responsibility of Southeast University.

https://doi.org/10.1016/j.foar.2023.07.001

Please cite this article as: A. Sepúlveda, S.S. Seyed Salehi, F. De Luca et al., Solar radiation-based method for early design stages to balance daylight and thermal comfort in office buildings, Frontiers of Architectural Research, https://doi.org/10.1016/j.foar.2023.07.001

1. Introduction

The building sector is one of the main reasons of global warming as it is responsible for 30% of the total Greenhouse Gas emissions (Wei et al., 2018). Moreover, buildings' energy needs account for 40% of the total energy consumed in Europe (Ahmad et al., 2014). Indeed, the Member States are encouraged by the Energy Performance of Buildings Directive 2010/31/EU (EPBD) to define specific requirements for new buildings (starting from January 1, 2021) to become nearly zero-energy buildings (nZEBs) (European Commission, 2010). In consideration of occupants visual comfort, the European standard EN 17037:2018 "Daylight in buildings" defined methods to quantify the level of different daylight aspects: sunlight exposure or solar access, view out, daylight provision, and glare protection (European Commission, 2018). Daylight provision has been proven crucial to balance humans' circadian rhythm (Duffy and Czeisler, 2009; Lockley, 2009). Indeed, daylight is the most preferred light source by building occupants (Knoop et al., 2019). During the COVID-19 pandemic, building occupants became more aware about how daylight in indoor spaces (considered as one environmental factor related to visual quality) can influence their psychological and physical well-being (Batool et al., 2021). Nowadays, facades with high window-to-wall ratios (*WWR*s) are a common solution at northern latitudes due to the lack of sun hours during the winter and the importance of the view to the outside (Thalfeldt et al., 2013). Nevertheless, the excess of daylight, for instance, caused by the presence of direct sunlight (despite of its importance on human health (Samuels, 1990)) can provoke summer thermal discomfort (Simson, 2019) and visual glare discomfort which is a complex phenomenon that depends on several factors such as the viewing direction, view position, luminance distribution and contrast, weather conditions, and external obstructions (Osterhaus, 2005). Indeed, relationship was observed between lighting level satisfaction and perceived thermal comfort, whereas the overall comfort depends more on thermal conditions than the lighting level (Fakhari et al., 2021). In addition, the balance between energy consumption and visual comfort in highly glazed buildings with adaptive biomimetic facades was proved feasible (Sheikh and Asghar, 2019). Facade design in urban canyons, which are characterized by homogeneous high obstruction levels, are challenging for architects and designers: the fulfillment of daylight provision requirements in high-obstructed lower floors and the minimization of cooling capacity (directly related to the draught risk) of low-obstructed higher floors are difficult to obtain with the same design parameters. Thus, floor dependent facade design decisions in the early design stages are needed to meet both, daylight and thermal comfort requirements while avoiding additional costs required by future renovations (Sepúlveda, 2022).

1.1. Balancing energy performance and daylight in buildings

The proposal of facades Multi-objective simulation methods were commonly used in previous investigations to achieve efficient building/facade level design decisions: Chen et al. (Pilechiha et al., 2020) found that the use of an efficient cooling system has the potential to achieve better trade-offs between energy performance and daylight provision in offices located in Singapore, and Konis et al. (2016) achieved the simultaneous increase of daylight provision (27%—65%) and decrease of Energy Use Intensity (EUI) (4%—17%) depending on the climate (Helsinki, New York, Los Angeles, Mexico city) by using its proposed Passive Performance Optimization Framework (PPOF).

Other studies used standard simulation methods based on validated softwares (EnergyPlus, DAYSIM, E-Quest) to propose efficient design decisions to balance energy and daylight during the facade design phase of different type of buildings located in low latitudes (25.762°—34.052°) (Li et al., 2016; Shen and Tzempelikos, 2012; Shishegar and Boubekri, 2017). Shen and Tzempelikos (2012) proved on one hand, that visible transmittance higher than 50% have the ability to allow enough daylight provision for *WWR*s higher than 50%, on the other hand, *WWR*s between 30% and 50% can result in lower energy consumption. Li et al. (2016) found that Building Integrated Solar Thermal Shading (BISTS) can effectively improve daylight provision in single perimeter office room by increasing the Useful Daylight Illuminance level (i.e., between 100 lux and 2000 lux) while achieving a 5.3% reduction of the primary energy use. Shishegar and Boubekri (2017) found that, for hot and arid climates, a *WWR* of 40% provides the highest electrical energy savings almost independently of artificial lighting control.

Regarding studies that considered multi-objective optimization (MOO) methods, Pilechiha et al. (2020) showed that their framework (to select room/window dimensions) could improve daylight provision and view out for more than 80% of the utilized south-oriented office room area while decreasing EUI about 12%. In addition, Naji et al. (2021) who proposed and used a MOO method to minimize thermal/visual discomfort and life cycle costs (LCC) of residential buildings located in the Australian context, found that the optimal solutions were unique for each climate zone: 27%—31% of energy savings and 6%—55% reduction of thermal comfort discomfort hours (compared to the baseline).

Several investigations proposed rules of thumb for facade design for different building types located at high latitudes (De Luca et al., 2022; Thalfeldt et al., 2013; Vanhoutteghem et al., 2015). Vanhoutteghem et al. (2015) highlighted the difficulties to achieve a good balance between daylight provision, energy consumption, and overheating protection in nZEB Danish single-family homes: low g-values and high visible transmittance values were recommended for south-oriented rooms and high g-values for north-facing windows to reduce the heating demand. Within the Estonian context, the optimal energy performance, costs and daylight are related to office buildings with highly transparent triple glazing systems (*WWR* of 40%) (Thalfeldt et al., 2013). De Luca et al. (2022) found through parametric analyses that static shadings can reduce visual discomfort by up to 89.8%, primary energy use by up to 29.1%, and provide adequate levels of daylight and view out for two existing NE/SE-oriented classrooms located in Tallinn, Estonia.

1.2. Design recommendations for Estonian offices

Currently in Estonia, there is a local standard EVS-EN 17037:2019+A1:2021 (Estonian Centre for Standardisation and Accreditation (Non-Profit Association), 2022) in line with the EN 17037:2018 (European Commission, 2018) (based on minimum Daylight Factor (min*DF*) and Spatial Daylight Autonomy (*sDA*) metrics). A recent investigation proved the reliability of the EN 17037:2018 (i.e., method 1: min*DF* criterion), through the comparison with the well-stablished method LM-83-12 based on the *sDA* metric (Illuminating Engineering SocietyThe Daylight Metric Committee, 2013), against the Estonian standard EVS 894:2008/A2:2015 (Sepúlveda et al., 2020). Regarding energy efficiency in buildings, Estonia has clear regulations that define the concept of Nearly Energy Zero Buildings (NZEB), assessment methodologies, and requirements based on the primary energy (Estonian Government, 2012, 2015).

Typically, office buildings in Estonia have active cooling systems because it is normally not possible to protect against overheating risk during the warm season only with hybrid (i.e., mechanical and natural) ventilation (Simson, 2019) due to the high level of internal gains that must be considered according to the Estonian regulation (Estonian Government, 2015), and to the possible solar gains. Therefore, a wrong combination of *WWR*, room dimensions, glazing type (visible transmittance: Tvis and total solar energy transmittance: g-value) and orientation/external obstructions of the office room could be detrimental not only for the energy performance (Thalfeldt, 2016), but also for the daylight provision (Sepúlveda et al., 2022a). For instance, Pikas et al. (Kurnitski et al., 2013) found that photovoltaic panels to generate electricity in Estonian office building would be necessary to achieve NZEB requirements despite of not being a cost optimal solution in 2014. In Estonian office buildings, which are typically very well insulated, the main factors of influence of the cooling capacity were the internal and solar heat gains due to the small differences between cooling set point and outdoor temperature (Seyed Salehi et al., 2021). Moreover, the higher solar heat gains related to high incident solar radiation levels are normally caused by low sun altitudes and sunny days (e.g., during spring/autumn) leading to an increase of the building's cooling capacity to maintain indoor set points. Higher air velocity (required to reach higher cooling capacity) in occupied zone is easily perceived as draught, which causes occupant dissatisfaction and complaints, as well as decrease in the productivity or effectively useable floor space area (Kiil et al., 2019). In fact, Kiil et al. (2020) demonstrated that high *WWR*s result in higher cooling loads and increase the need for larger room cooling units, higher cooled airflow rates or lower supply air temperatures to achieve a cooling set point, the latter factors also increasing the risk of draught in occupied office spaces.

1.3. Novelty and objectives of this investigation

In 2005, Li et al. (2005) applied regression analyses to predict the increment of cooling energy in an office room located in Hong Kong, China from the incident solar radiation and *WWR*·Tvis (common design parameter in early design stages). However, this prediction method does not consider different g-values of the glazing system or obstruction angles of the surrounding buildings, which can have a crucial impact on the predicted cooling energy increment. Although previous investigations proposed optimization workflows (Chen et al., 2018; Huang et al., 2021; Konis et al., 2016; Pilechiha et al., 2020) and rules of thumb (De Luca et al., 2022; Thalfeldt et al., 2013; Vanhoutteghem et al., 2015) to balance energy performance and daylight in buildings during early design stages, there is a lack of: (1) consideration of the obstruction angle as independent variable; and (2) the simulation-free prediction methods to design office buildings with a desired thermal comfort level (affected by the specific cooling capacity *SCC*). Thus, the consideration of different obstruction angles is important to propose easy-to-use prediction methods for architects and designers to design office buildings located in urban canyons. Thus, there is a need to understand correlation between obstruction angle and incident solar radiation/daylight provision/cooling capacity for different facade orientations (e.g., South: S, South-east: SE, East: E, North-east: NE, North: N, North-west: NW, West: W, South-west: SW) to balance daylight and thermal comfort in office buildings, especially in cold climates where there is a poor daylight availability during the cold season, and high thermal mass constructions. In order to fill this research gap, the main aim of this investigation is to develop an easy-to use solar radiation-based prediction method for the design of office buildings facades (i.e., decisions: room size, window-to-floor ratio: *WFR*, Tvis, g-value) located in urban canyons to balance daylight provision according to the EN 17037:2018 and thermal comfort. Firstly, the scientific novelty of this investigation lays on the correlation study between the mentioned design variables and building performances (*sDA* and *SCC*). Secondly, the development of prediction methods can help architects and designers to work more efficiently during early design stages and to obtain more performative solutions in shorter time. To fulfill the aims of the study, the objectives of this investigation are as follows:

- O1: To develop a solar radiation-based prediction method for *WFR*·Tvis based on obstruction angle-incident solar radiation to fulfill daylight provision according to method 2 defined by the EN 17037:2018;
- O2: To develop a solar radiation-based prediction method for *WFR*·g-values based on obstruction angle-incident solar radiation to ensure a certain level of thermal comfort through controlling *SCC*;
- O3: To propose design workflows based solar radiation-based prediction methods for the early stage design of facades in future office buildings in Estonia;
- O4: To validate the proposed design workflow through its application to design an office-building facade initial solutions in Tallinn, Estonia.

2. Methodology

In order to achieve the objectives of this investigation (O1—O4), we used a simulation-based approach (Fig. 1):

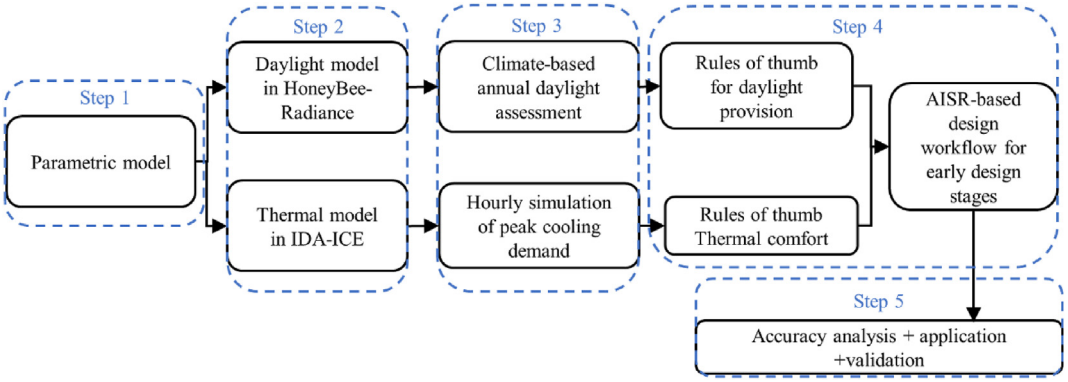

Fig. 1 Flowchart of the methodology used in this investigation.

1) Creation of the parametric model of a generic office room (Section 2.1);
2) Set up daylight (Section 2.2) and thermal (Section 2.3) parametric models including different visible transmittances (Tvis) and g-values related to different glazing types;
3) Annual assessment of daylight provision according to method 2 proposed in the EN 17037:2018 (Section 3) and *SCC* (Section 4);
4) Analysis of the annual assessment results to generate easy-to-use rules of thumb to balance daylight provision (O1, Section 3.1) and thermal comfort (O2, Section 3.2);
5) The application and validation of the proposed solar radiation-based workflow (O3) to balance daylight and thermal comfort in a new office building development project within Estonia (Section 3.3–3.5).

2.1. Parametric model of a generic single office

We used a simulation-based methodology with a single-zone approach for the assessment of daylight provision and *SCC*. Thus, we built a parametric model of a generic office room in GH for Rhinoceros. The range for all the design parameters considered in the parametric model can be seen in Fig. 2. The independent variables or design parameters of the parametric model are: room orientation (*ro*), room width (*rw*), room depth (*rd*), window width (*ww*), window height (*wh*), and obstruction angle (θ). The dependent variables are *sDA* (%) and *SCC* (W/m^2).

Since the case studies are located in Tallinn, Estonia (Lat. 59°26′N, Lon. 24°45′E, humid continental climate according to Köppen-Geiger classification DFb (Peel et al., 2007)), we used a building typology already used in previous investigation within the Estonian context (Sepúlveda et al., 2020, 2022a). The room dimensions (*rw*: 3.5—6.5 m, *rd*: 3.5—7.5 m, room height: 3 m) and number of orientations were selected to obtain a representative sample of typical office rooms in Estonia. The small 3.5 m × 3.5 m rooms represent a single office of approximately 12 m^2. Room areas of 20—40 m^2 represent medium-size offices. Rooms with a size of 6.5 m × 7.5 m represent large offices of ~50 m^2. The total number of room combinations is 61,440 for *sDA* and *SCC* simulations.

We set the maximum width of 1.75 m for a single glazed area. Thus, the number of vertical window dividers was varied from 0 (*ww* = 1.75 m) to 3 (*ww* = 5.655 m) (Fig. 3 (a)). The frame width (4.3—6.6 cm) was calculated to ensure a constant frame ratio of 12% (Fig. 3 (a) and (b)). In Fig. 3 (c), different room combinations have the same

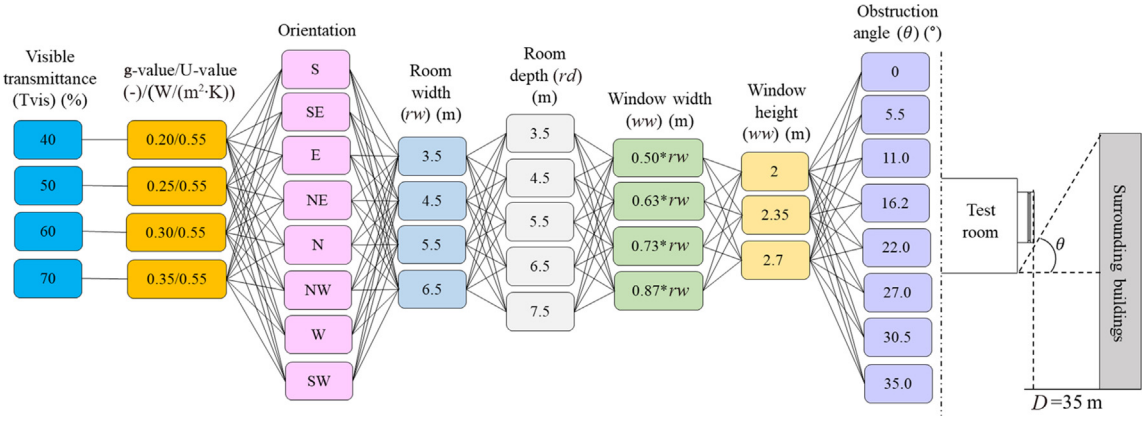

Fig. 2 Diagram of room parameter combinations and representation of the obstruction angle θ for a generic room. An obstruction angle is considered null ($\theta = 0°$) when the roof of the surrounding building/external obstruction is at the same level or below the floor level of the test room.

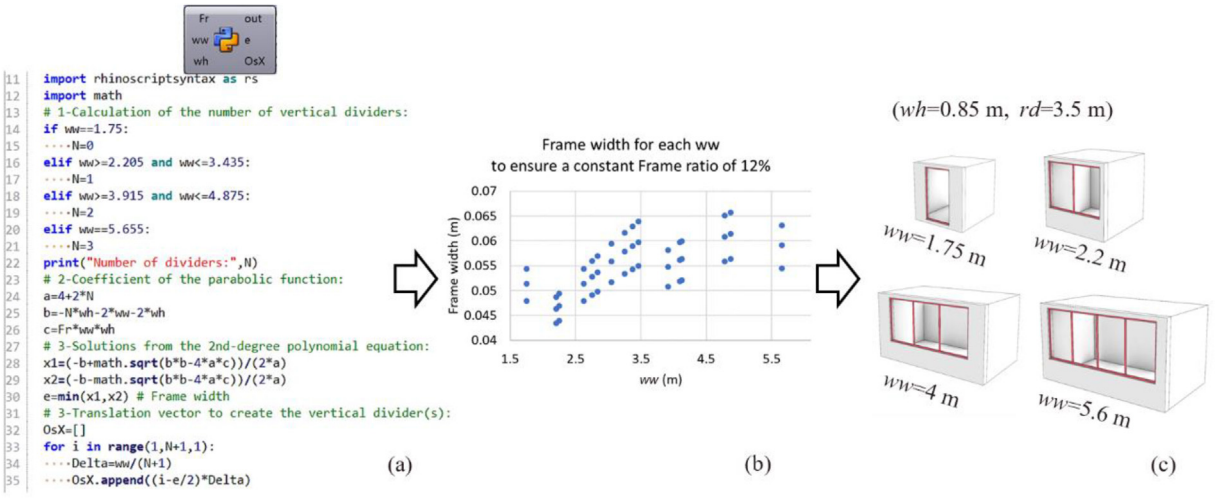

Fig. 3 Algorithm to calculate the frame width (*e*) to ensure a specific frame ratio (*Fr*) of 12% depending on the window width (*ww*). (a) Frame width-*ww* combinations for the generated room combinations; (b) Room combinations with different *ww* values and constant window bottom-sill height (*wh*) of 0.85 m; (c) Delta (distance) between vertical dividers and OsX (ranslation vector) to generate each window frame divider.

frame ratio despite of the different *ww* and number of dividers to ensure the structural feasibility of the fenestration system. The window top-ceiling distance was fixed to 0.15 m and the window heights were 2 m, 2.35 m, and 2.7 m corresponding to a windowsill height of 0.85 m, 0.5 m, and 0.15 m, respectively. Thus, considering all the room and window sizes, *WFR* varied from 13.3% to 67.1%.

The distance between the external facade of the test room and the surrounding building was set to 35 m, which represents the worst-case scenario for daylight provision (for the same obstruction angle), i.e., minimum availability of diffuse (from the sky) and reflected light to the indoor space due to closer luminance sources (light reflected by the surrounding buildings). In order to model an urban canyon, the opposite building was modelled as continuous facade and the height was varied to simulate the mean obstruction angle (θ) from 0° to 35.0° (Fig. 2) as considered in previous research (Sepúlveda et al., 2022a). As triple glazing systems are a common and cost-optimal design solution within the Estonian context, we considered a fixed total thermal transmittance (U-value) of 0.55 W/(m^2·K) (Thalfeldt et al., 2013, 2017). The visible transmittance of the glazing system was varied from 40% to 70%. The g-values were varied from 0.20 to 0.35 (Fig. 2) to consider triple-glazing systems in the market with a Tvis-g-value ratio of 2 (LSG = 2) (Lee et al., 2022), maximizing the potential balance between daylight provision and *SCC* in all the generated rooms (Sepúlveda et al., 2022a). Finally, we did not consider shading systems in our parametric model because they can be considered in later stages of facade design only (cost-efficiency) if predicted size of glazed areas required to fulfill daylight requirements is larger than maximum size of glazed areas required to control *SCC*.

2.2. Daylight provision assessment

In early design stages the consideration of daylight is more suitable than glare protection as stated by Sepúlveda (2022): glare protection issues and further tuning of window properties and shading should be solved during the next design stages. For each generated room combination we assessed daylight provision according to method 2 defined by the EN 17037:2018: based on *sDA* (European Commission, 2018). The reference plane was located at 0.85 m from the room floor level as defined by the EN 17037:2018. In addition, as recommended by the standard 0.5 m × 0.5 m grid cells were considered for the calculation of horizontal illuminance values. The offset distance between the grid points and the room walls was 0.5 m in order to avoid unrealistic low illuminance values due to the common presence of furniture close to the interior walls. The reflectance values of the window frame were set to 0.5 corresponding to a silver aluminum window frame and the reflectance values of the opaque surfaces were set according to standard values defined in the EN 17037:2018 (Table 1).

According to method 2, a minimum, medium, and high level of recommendations for daylight provision correspond to the simultaneous fulfillment of $sDA_{100,50}\geq 95\%$ and $sDA_{300,50}\geq 50\%$, $sDA_{300,50}\geq 95\%$ and $sDA_{500,50}\geq 50\%$, and $sDA_{500,50}\geq 95\%$ and $sDA_{750,50}\geq 50\%$, respectively (Table 2). As for annual climate-based daylight simulations such as the

Table 1 Reflectance (*R*) values for opaque surfaces recommended by the EN17037 for daylight simulations (European Commission, 2018).

Surface	Reflectance (0–1)	Surface	Reflectance (0–1)
Interior walls	0.5	External ground	0.2
Floor	0.2	External facade and buildings	0.3
Ceiling	0.7		

DA simulations, we used the matrix-based method called "2-phase method" implemented in the component "HB Annual Daylight", which has been proved reliable for annual daylighting calculations with conventional fenestration systems such as the glazing we have in our daylight models (Subramaniam, 2017). Thus, we used the Radiance parameters show in Table 3 (Sepúlveda et al., 2022b).

Table 3 Radiance parameters used for annual daylight simulations in HoneyBee-Radiance (Sepúlveda et al., 2022b).

Radiance parameter	Value
Ambient bounces (*-ab*)	6
Ambient divisions (*-ad*)	25,000
Ambient super-samples (*-as*)	4096
Sampling (*-c*)	1
Direct certainty (*-dc*)	0.75
Direct pretest density (*-dp*)	512
Specular threshold (*-st*)	0.15
Direct relays (*-dr*)	3
Source substructuring (*-ds*)	0.05
Direct thresholding (*-dt*)	0.15
Limit reflection (*-lr*)	8
Limit weight (*-lw*)	4e-07
Specular sampling (*-ss*)	1.0

2.3. Thermal comfort assessment

The Estonian regulations set the summer-time over-heating requirements for new buildings and their fulfillment is the prerequisite for not installing a mechanical cooling system (Riigi Teataja, 2020). The requirements stipulate the maximum number of degree-hours in critical rooms of a building over limit temperature, which for residential and non-residential buildings are 27 °C and 150 °Ch, 25 °C and 100 °Ch, respectively. Rules of thumb for fulfilling both daylight and over-heating requirements in apartment buildings were developed by Sepúlveda et al. (2020). However, the limit temperature 25 °C and the degree-hour threshold 100 °Ch in non-residential buildings are significantly stricter than in residential buildings. Additionally, the internal gains in non-residential buildings are larger than residential buildings, which in practice obligates controlling the room temperatures by installation of mechanical cooling systems.

Assuring thermal comfort in ventilated spaces requires controlling both the room temperature and air velocity to diminish complaints (Fanger and Christensen, 1986) and too high air velocities are in practice often the cause for complaints even when the air temperature is within required limits (Hens, 2009; Kähkönen, 1991). Typically, cooling panels, thermally activated buildings systems (TABS), active chilled beams and fan-coil units are used for room cooling in Estonia. Kiil et al. (2020) conducted a thorough field-study of air temperature and air velocities in office buildings during cooling season where each of these systems were installed. They concluded that in buildings with radiant cooling panels, TABS and active chilled beams indoor climate category remained in between I (high level) and II (medium level), whereas the building with fan-coils and largest *SCC* performed worst and the indoor climate category III (minimum level) was reached. Additionally, the building with cooling panels and lowest *SCC* performed best and indoor climate category I was reached in most rooms. Although, good indoor environment requires careful design and proper installation of mechanical cooling, the prerequisite of assuring thermal comfort is well controlled *SCC*. Therefore, in this study the recommended thermal comfort levels are defined through *SCC*.

The best performing currently available common cooling system is with radiant cooling panels, but since there is no forced convective air flow in these systems, their cooling capacity is limited. Võsa et al. (Karl-Villem et al., 2022) measured the performance of cooling panels and Salehi et al. (2022) validated the thermal model and concluded that the real nominal cooling output of the panels k_c corresponded well with the values provided in the technical documentation. The maximum *SCC* cooling capacity of radiant cooling panels can be calculated based on the parameters of cooling panels (Zehnder Baltics OÜ, 2018) and typical design parameters of cooling systems as follows:

$$\Phi_{\text{specific,max}} = CP_{\text{area,specific,max}} \cdot k_{\text{c,specific}} \cdot \left(\frac{t_{\text{ret}} - t_{\text{sup}}}{\ln\left(\frac{t_{\text{sup}} - t_{\text{a}}}{t_{\text{ret}} - t_{\text{a}}}\right)} \right)$$

where $\Phi_{\text{specific,max}}$ is the maximum *SCC* (W/m^2), $CP_{\text{area,specific,max}}$ is the maximum cooling panel area per room floor area (0.5), $k_{\text{c,specific}}$ is nominal cooling output per panel area (9.98 W/K/m^2), t_{ret} is design return temperature of cooling system (18 °C), t_{sup} is design supply temperature of cooling system (15 °C) and t_{a} is design room temperature for cooling (25 °C). The resulting maximum *SCC* with cooling panels is thus 39.9 W/m^2. As Kiil et al. (2020) showed, the active chilled beams are a suitable cooling solution for

Table 2 Recommendations of daylight provision by daylight vertical openings according to the EN 17037:2018 (European Commission, 2018).

Level of recommendation	Target illuminance E_T (lux)	Fraction of space for target level $F_{\text{plane, \%}}$ (%)	Minimum target illuminance E_{TM} (lux)/DF (%)	Fraction of space for minimum level $F_{\text{plane, \%}}$ (%)	Fraction of daylight hours, $F_{\text{time, \%}}$ (%)
Minimum	300	50	100	95	50
Medium	500	50	300	95	50
High	750	50	500	95	50

assuring indoor climate category II and REHVA Guidebook No. 5 (Virta et al., 2007) suggested optimal *SCC* between 60 and 80 W/m^2 for active chilled beams. Based on the presented information, the *SCC* limits for different comfort levels used in this study are the following: minimum, medium, and high for a maximum *SCC* of 80, 60, and 40 W/m^2, respectively.

2.4. Thermal model

The thickness of interior walls and ceilings were constant and construction materials thermal properties were adjusted (Domínguez-Muñoz et al., 2010) to achieve thermal performance related to heavy construction type used in previous research (Seyed Salehi et al., 2021) (Table 4). The window constructions with a constant LSG ratio of 2 are shown in Table 5.

Slab floor and interior walls were considered as adiabatic surfaces as it is a typical boundary condition for office rooms energy simulations. However, we considered heat transfer through the exterior wall and solar exposure and the thermal mass of the interior surfaces was accounted for in the simulations. Required usage profiles for internal gains in office buildings (same for occupancy, lighting, and equipment) by Estonian regulations can be seen in Fig. 4. For a single office, the area per person is 10.0 m^2 and the mean level of activity is 1.2 met (Table 6). HVAC settings used in our thermal model are displayed in Table 6. Ideal coolers controlled with proportional-integral (PI) controllers were used as room units to model the cooling capacities. Mechanical ventilation was also considered: minimum fresh air of 1.4 L/sm^2 during occupied hours (CEN, 2019). Additionally, the ventilation airflow rate of a non-residential building is deemed to be 0.15 L/sm^2 during unoccupied hours. Although dimming control has been more used in new Estonian office buildings during the past years, peak cooling load for sizing cooling room units was calculated in this study and typical ON/OFF control with predefined schedule was assumed in these calculations for a safety margin. It cannot be assured that the occupant does not draw interior blinds when peak cooling load occurs and thus, it triggers the operation of the lighting system on full power. As the focus of this study is on early-stage design and many rough estimations need to be done, smart controls for lighting system and blinds can be used to reduce peak cooling loads in latter design stages if needed to simultaneously reach high daylight and thermal comfort levels.

Table 5 Windows glazing specifications.

Parameter	Type 1	Type 2	Type 3	Type 4
Solar heat gain coef. (SHGC) (0—1)	0.2	0.25	0.3	0.35
T. Solar transmittance (0—1)	0.17	0.21	0.25	0.3
Visible transmittance, Tvis (%)	40	50	60	70

Note: Internal emissivity = External emissivity = 0.9, Glazing U-value = 0.55 W/(m^2·K).

3. Results and discussion

3.1. Minimum *WFR*·Tvis to ensure a specific daylight provision class

The aim of this section is to develop a solar radiation-based prediction method for minimum *WFR*·Tvis depending on annual incident solar radiation (AISR) related to the external facade of the office room to fulfill different levels of daylight provision according to the method 2 defined by the EN 17307:2018. We define the metric minimum *WFR*·Tvis (min*WFR*·Tvis) as the main design variable to achieve a certain level of daylight provision, since it includes all the design parameters affecting daylight provision. As can be seen in Fig. 5, the level of obstruction can be correlated to the AISR that the center of the external facade receives during the whole annual period (as considered for $sDA_{x,50}$ calculations), which represents an useful design input for the designer during the building massing stage (Sepúlveda and De luca, 2020).

In Fig. 6, the linear correlation coefficient R^2 for different AISR values, room orientation, and illuminance threshold *x* is shown. Since there is not strong correlation

Table 4 Thermal properties of the building envelope.

Element	Construction	Total Thermal transmittance (W/(m^2·K))	Layer density (kg/m^3)	Layer Specific Heat (J/(kg·K))	Layer Thermal conductivity (W/(m·K))
External wall	Render 10 mm	0.128	1800	790	0.8
	Concrete 150 mm		2300	880	1.7
	Expanded Polys. 270 mm		20	750	0.036
	Concrete 50 mm		2300	880	1.7
Slabs	Floor coating 5 mm	0.2	1100	920	0.18
	Concrete slab 150 mm		2300	880	1.7
	Insulation 245 mm		92	2010	0.052
Internal walls	Concrete 150 mm	3.8	2300	880	1.7
Window frame	Aluminium 50 mm	2	450	900	0.1

Note: Polys.—Polystyrene.

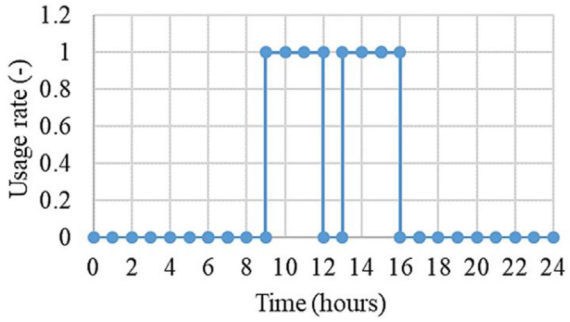

Fig. 4 Usage profiles of occupancy, lighting, and equipment for a single office in Estonia (Estonian Government, 2015).

($R^2 < 0.90$) between $sDA_{x,50}$ and AISR for almost all the illuminance thresholds (100 lx, 300 lx, and 500 lx), $sDA_{100\text{-}500,50}$ cannot be predicted with linear fitting. Therefore, the development of $sDA_{100-500,50}$ prediction formulas are not viable in terms of accuracy as the min*DF*-based one developed by Sepúlveda et al. (2022a).

Moreover, designers might prefer to work with simple solar radiation-based prediction methods to achieve a certain level of recommendation according to the EN 17037:2018. Specifically, for each *WFR*·Tvis, the minimum $sDA_{x,50}$ is searched (orange circles in Fig. 7 related to the most conservative daylight level for each *WFR*·Tvis) in order to ensure the fulfillment of a desired level of daylight provision based on $sDA_{x,50}$ thresholds (Table 2). Then, the min*WFR*·$Tvis_{50}$ and min*WFR*·$Tvis_{95}$ is the minimum *WFR*·Tvis, for which minimum $sDA_{x,50}$ is higher than 50% (red dotted lines represent the threshold for target level) and 95% (green dotted lines represent the threshold for minimum target level), respectively (Fig. 7).

Recommendations for min*WFR*·$Tvis_{50}$ and min*WFR*·$Tvis_{95}$ can be made for different illuminance thresholds (i.e., *x* values) (Fig. 8(a) and (b)). Moreover, considering the definition of daylight provision classes defined in Table 2 and the min*WFR*·$Tvis_{50\text{-}95}$ values, the solar radiation-based prediction method for daylight provision can be represented graphically (e.g., for south-oriented rooms, see Fig. 8(c)). According to this prediction method to achieve a minimum level of daylight provision (Fig. 9(a)), the min*WFR*·Tvis recommended value for any orientation is between 0.1 and 0.25 for θ between 0° and 35°, respectively. For a medium level of recommendation (Fig. 9(b)), the min*WFR*·Tvis value for any orientation should be between 0.225 and 0.4 for θ between 0° and 35°, respectively.

Table 6 Internal gain parameters for Estonian single office.

Parameter	Value
People density	0.1 p/m^2
Metabolic Rate	1.2 met
Equipment power density	12 W/m^2
Lighting power density	6 W/m^2
Lighting control	ON/OFF
Target Illuminance	500 lux

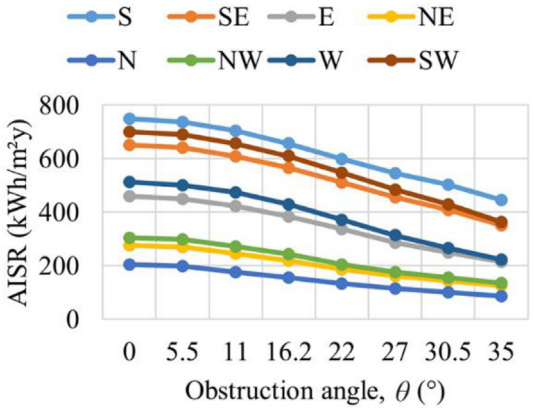

Fig. 5 Accumulated AISR for different room orientations and obstruction angles. AISR values were calculated in a 1 m × 1 m surface located at the center of the external facade of the room.

Finally, to achieve a high level of recommendation (Fig. 9(c)), the min*WFR*·Tvis value for any orientation should be between 0.30 and 0.475 for θ between 0° and 35°, respectively.

3.2. Maximum *WFR*·g-values to ensure a specific thermal comfort class

The aim of this section is to develop a solar radiation-based prediction method for maximum *WFR*·g-value (max*WFR*·g-value) depending on the AISR of the office room to fulfill different levels of thermal comfort level. We propose the metric maximum *WFR*·g-value to achieve a certain level of thermal comfort class (minimum, medium, or high) as the main design variable, since it includes room dimensions (*rw* and *rd*), window dimensions (*ww* and *wh*), and g-*value*. Thus, max*WFR*·g-value recommendation depends on *ro*, θ and the construction materials of the room.

In Fig. 10(a), the linear correlation coefficient R^2 for different AISR values, room orientation, and *SCC* values is shown. Since there is a strong correlation ($R^2 \geq 0.97$) between *SCC* and AISR for all the orientations and both construction materials, *SCC* can be predicted with linear fitting. However, a solar radiation-based prediction method considering not exceeding max*WFR*·g-value of 80, 60, 40 W/m^2 represent the simplest, most accurate, and conservative design recommendations. Once *SCC* results were obtained from annual energy simulations with IDA-ICE software, for each *WFR*·g-value the maximum *SCC* value is searched (orange circles in Fig. 10(b)). Then, we indicated with max*WFR*·*g*-$value_{80}$, max*WFR*·*g*-$value_{60}$, and max*WFR*·*g*-$value_{40}$, the max*WFR*·g-value, whose minimum *SCC* does not exceed 80, 60, and 40 W/m^2, respectively (Fig. 10(b)).

Once max*WFR*·g-$value_{80}$, max*WFR*·g-$value_{60}$, and max*WFR*·g-$value_{40}$ were obtained for both construction materials, we can build rules of thumb for different room orientation and AISR (Fig. 11). According to the rules of thumb to achieve any level of thermal comfort, the

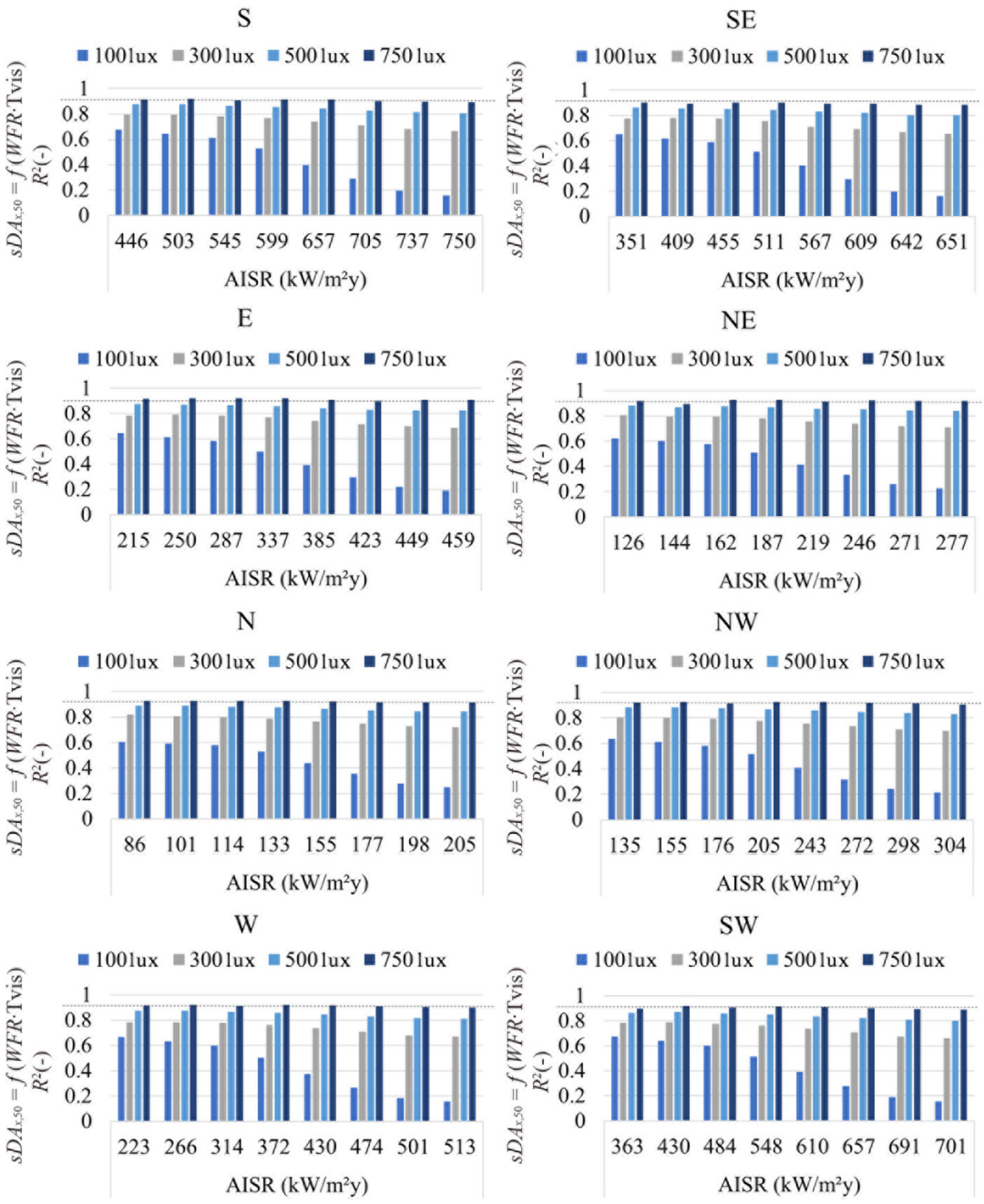

Fig. 6 Correlation coefficient R^2 between $sDA_{x,50}$ and $WFR \cdot Tvis$ for different AISR values, room orientations, and illuminance thresholds x (100, 300, 500, and 750 lux).

maximum recommended max*WFR*·g-value is 0.18 and it is related to north-oriented concrete-based office rooms. The most critical room orientation is S as it is related to the minimum (most restrictive) max*WFR*·g-values: 0.16, 0.12, and 0.08 to achieve a minimum, medium, and high level of thermal comfort in concrete-based office rooms.

3.3. Prediction accuracy of the solar radiation-based prediction methods

The aim of this section is to quantify the level accuracy of the solar radiation-based prediction methods to predict level of fulfillment for daylight provision and thermal comfort classes. We consider the percentage of room combinations whose level of daylight provision and thermal comfort are correctly, under (conservative prediction), and wrongly predicted. The design workflow selected was the second one, for which Tvis and g-value are input and min*WFR* and max*WFR* are calculated. We used the design workflow 2 that was implemented as open-source tool, and modified it to compare the calculated mean*WFR* from min*WFR* and max*WFR* values (average value between min*WFR* *and* max*WFR*), which were obtained from daylight/thermal comfort prediction methods with actual *WFR* values.

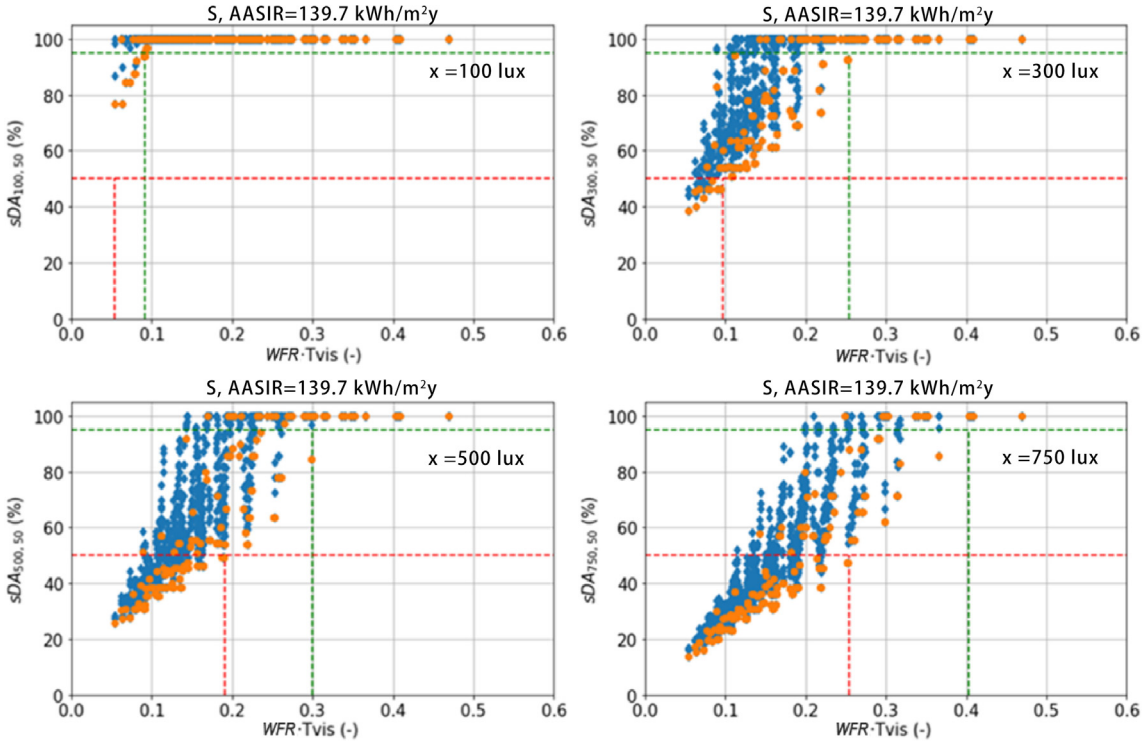

Fig. 7 Spatial Daylight Autonomy ($sDA_{x,50}$) for unobstructed ($\theta = 0°$, accumulated AISR = 139.7 kWh/m^{2}y) south-oriented room with different *WFR*·Tvis combinations and different illuminance thresholds (x = 100, 300, 500, 750 lux).

The level of prediction accuracy for different level of thermal comfort and daylight provision is shown in Fig. 12. The maximum percentage of wrong predictions, in any case, is less than 2.5% (Concrete-based construction, high level of thermal comfort). The mean percentage of right predictions of thermal comfort classes is high; 98.7% and 98.8% for rooms with concrete-based rooms, respectively. This high accuracy is due to the high level of correlation between *SCC* and max*WFR*·g-value (Fig. 6). The existence of wrong predictions could be due to arithmetical errors when subtracting min*WFR* to max*WFR* values for each room (e.g., absolute differences of 1e-3). The mean percentage of right predictions of minimum, medium, and high level of daylight provision is 100%, 75.6%, and 88.7%, respectively. This low accuracy (for medium and high level) is due to a combination of two decisions: (1) the low level of correlation between *sDA* and min*WFR*·Tvis and (2) the conservative selection approach that we used to define the min*WFR*·Tvis for each AISR value (Fig. 9). Moreover, it was expectable to have much more number of conservative than wrong prediction (Fig. 12) specifically because the later decision to generate the rules of thumbs. This accuracy analysis tells that in order to achieve a medium or high level of daylight provision, the proposed prediction model might not be reliable enough if the designer does not accept conservative predictions.

For the prediction of daylight classes, the percentage of conservative recommendations is higher than wrong predictions: up to 23.9% versus 0.64%. Moreover, the existence of wrong predictions could be due to arithmetical residuals when subtracting min*WFR* and max*WFR* values for each room (e.g., absolute differences of 1e-3) as well as the existence of double-threshold requirements for the *sDA* metric (Table 2), whereas the *SCC* does only have one threshold per thermal class defined in Section 2.3. In summary, we can determine that solar radiation-based prediction methods could be accurate, depending on the accepted level of accuracy needed, thermal classes, and daylight classes considered. In overall, the probability to obtain a conservative prediction of the medium/high-level daylight classes of a room is 6.7% higher in absolute terms when using solar radiation-based prediction method for daylight provision. This analysis provides a sense of how well, the developed solar radiation-based prediction methods, can predict the different levels of daylight provision and thermal comfort in room combinations generated by our parametric model.

3.4. Design workflow(s) to balance thermal and visual comfort

Based on the presented solar radiation-based prediction methods for min*WFR*·Tvis and max*WFR*·g-value generated from the parametric model, we propose two main design workflows to be used by architects and designers during early design stages. The main design workflow consists of four steps (Fig. 13):

1) Building massing and external facade generation (test surfaces representing possible room's location) according to the designer's criterion that might be influenced by factors such as client's requirements, aesthetics, construction materials, solar rights of the surrounding buildings (i.e., solar envelopes (De Luca and Dogan,

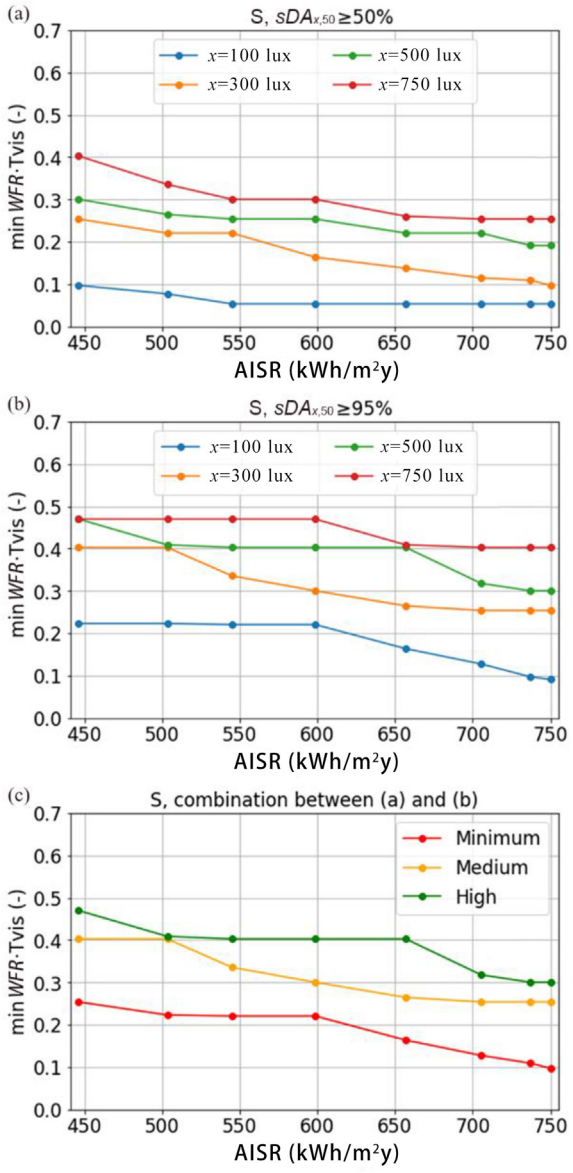

Fig. 8 Minimum recommended *WFR*·Tvis for south-oriented rooms depending on the accumulated AISR to achieve a $sDA_{x,50}$ of 50% (a), 95% (b), and different levels of recommendation of daylight provision (c) according to the method 2 (based on the *sDA*) defined by the EN 17037:2018.

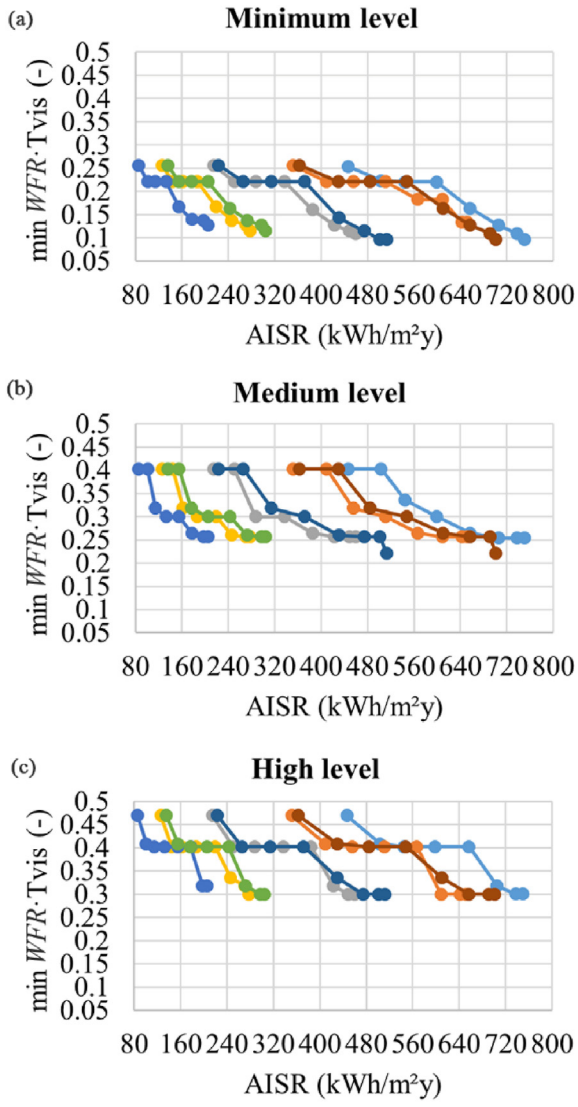

Fig. 9 Minimum recommended *WFR*·Tvis depending on the room orientation and the accumulated AISR to achieve a minimum (a), medium (b), and high (c) level of daylight provision according to the method 2 (based on the *sDA*) defined by the EN 17037:2018.

2019)), passive cooling and heating massing strategies (Sepúlveda and De Luca, 2022), accessibility, location of windows, required floor-area ratio, etc.

2) An annual solar simulation is needed to quantify the accumulated AISR for each test surface.
3) Firstly, for a desired level of recommendation for daylight provision, the selection of the min*WFR*·Tvis considering *sDA*-based criterion can be made (Fig. 9). Secondly, for a desired level of recommendation for thermal comfort, the selection of the max*WFR*·g-value (Fig. 11).
4) To use min*WFR*·Tvis and max*WFR*·g-value for each test surface as practical information for the designer.

3.5. Facade optimization case

The aim of this section is two-fold. On one side, we show how the solar radiation-based prediction methods could be applied for the facade optimization of an SE-oriented office building that will be developed in Tallinn, Estonia (design workflow 2: chosen *WFR* unknown glazing properties, Fig. 13). On the other side, detailed daylight and thermal simulations are conducted to quantify the level of reliability that the solar radiation-based prediction methods could have in existing case studies where the surrounding buildings do not represent an urban canyon. The building has a rectangular shape and an interior courtyard. The optimization problem consists of finding the properties of the glazing system (g-value and Tvis with an LSG of 2, as considered in our parametric model) and *WWR* for each of

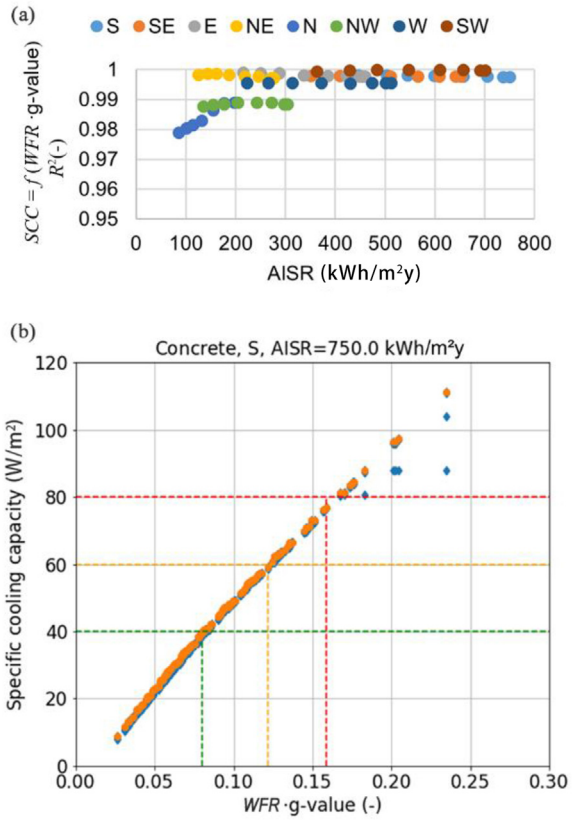

Fig. 10 Correlation coefficient R^2 between *SCC* and *WFR*·g-value for different AISR values and room orientations (a) and *SCC* for unobstructed ($\theta = 0°$, accumulated AISR = 750.0 kWh/m^{2}y) concrete (a) south-oriented room with different *WFR*·g-values combinations (b).

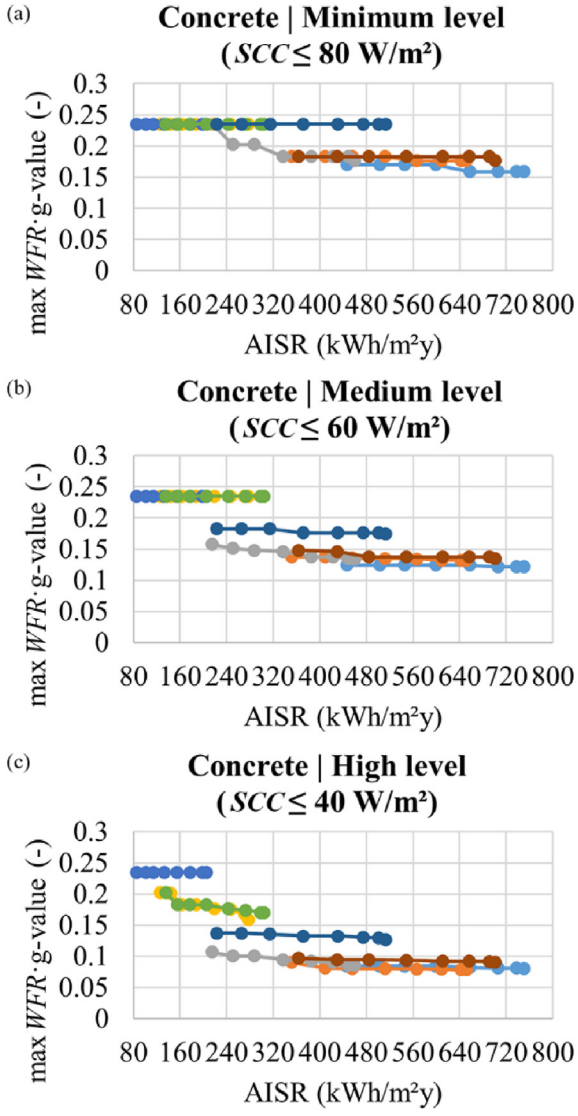

Fig. 11 Maximum recommended *WFR*·g-value depending on the room orientation and the accumulated AISR to achieve a minimum (a), medium (b), and high (c) level of thermal comfort.

the 162 test cells, which represents the potential location of medium size office rooms (5 m × 5 m).

The first step to optimize both facades is the solar radiation analysis (Fig. 14(a)). Note that there are test cells that are recognized by the workflow because the AISR (158 instead of 162) values are out of the range considered in the generated solar radiation-based prediction methods in this investigation, and therefore the validity of the recommendations whether to propose a min*WWR* or max*WWR* might be compromised. Specifically, one solar radiation analysis was conducted with LadyBug Tools to calculate AISR on each test cell, needed by solar radiation-based prediction method for daylight provision (to predict min-*WWR*·Tvis). In Fig. 14(a), the maximum AISR values are concentrated in the upper floors of the SE facade, the lowest values are related to lower floors, and the characteristic distribution is due to the skyline of the multi-tower neighboring buildings.

The optimal facade solutions to fulfill different combined requirements between thermal comfort and daylight provision were generated in less than 73,152 room combinations in 80 s (0.00109 s/room−1.1 ms/room) of computation time by using the developed open-source GH plug-in "HealthyFacadeGenerator" (Fig. 14(b–j)). The optimal facade solution for each design criteria combination has the maximum Technical Feasibility Ratio (*TFR*), which is the percentage of the room combinations whose *WWR* (calculated as the mean value between min*WWR* and max*WWR*) are between the minimum and maximum technically possible if considering the type of window dimensions of the parametric model explained in Section 2.1. The secondary criterion to select the optimal facade solution was the mean max*WWR*-min*WWR* (m*Wd*), which quantifies the selection margin the designer would have to select the *WWR* value. For instance, to achieve a minimum level of thermal comfort and a medium level of daylight provision, predicted optimal *WWR* values (with g-value = 0.29 and Tvis = 58%) are between 59% and 67% (Fig. 14 (k)), which correspond to low and high AISR values (Fig. 14 (a)).

For minimum, medium, high level of thermal comfort; *TFR* decreases with the daylight class: 100%, 100%, 52.5%; 100%, 93%, 0%; and 77.8%, 0%, 0% for a minimum, medium, and high level of daylight provision, respectively. Thus,

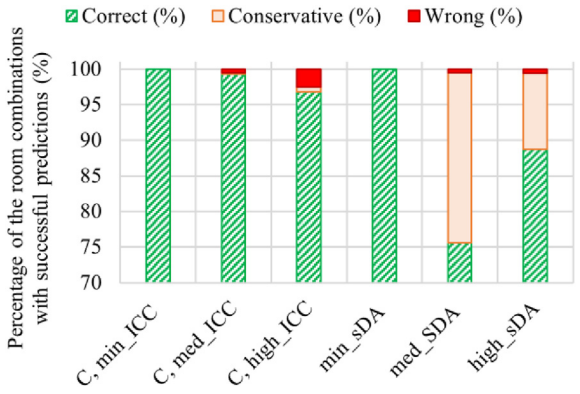

Fig. 12 Percentage room combinations (%) whose predicted thermal comfort/daylight provision levels by the solar radiation-based prediction methods for different construction types for interior walls and daylight criteria are correct, conservative, and wrong predicted. min = minimum, med = medium, *ICC* = thermal comfort class.

room facades with lower AISR become critical to fulfill medium and high level of daylight provision. Most of optimal g-values are 0.35 and the related Tvis values are 70%, meaning the achievement of certain level of daylight provision in this optimization case is more challenging than ensuring levels of thermal comfort for most of the design criteria. The higher daylight and/or thermal comfort requirements the more critical rooms located at first floors become, this is due to a combination of higher obstruction of the surrounding buildings and the south orientation of the building corner (Fig. 14 (d), (f) and (h)). In conclusion, fulfilling high-level daylight and thermal comfort simultaneously requires advanced facade solutions (i.e., dynamic shading) and/or careful cooling system design. For instance, rooms located in the bottom corner of the building could be used as rooms that do not have permanent occupancy and therefore are not critical from an indoor comfort perspective (Fig. 14 (d) and (f)). The accuracy of the method to predict the level of combined fulfillment can be seen in Fig. 15 (related to optimal cases shown in Fig. 14).

As can be seen, solar radiation-based prediction methods predicted medium-high *WWR*s, which in practice could be in conflict with energy efficiency during the cold season. Simulations of *sDA* and *SCC* were conducted for 158 rooms for each of the 9 design criteria and compared with predictions generated by the tool "HealthyFacadeGenerator":

- **In terms of daylight provision** (Fig. 15 (a) and (b)): In average, 65% of the prediction are correct (Design-*WWR*>min*WWR*). There are only wrong predictions when considering design criteria D0T2 and D1T2 with relative deviations below 22% (Fig. 14(b)). For a minimum level of thermal comfort, the agreement between predictions and actual building performance was 85.4%, 24.1%, and 22.2% for minimum, medium, and high level of daylight provision, respectively. For a medium level of thermal comfort, the agreement between predictions and actual building performance was 74.1%, 18.4%, and 100% for minimum, medium, and high level of daylight provision, respectively. For a high level of thermal comfort, the agreement between predictions and actual building performance was 69%, 90.5%, and 100% for minimum, medium, and high level of daylight provision, respectively. For design criteria different than D0T2 and D1T2, conservative predictions account up to 81.6% with a mean of 33.6%. Conservative predictions are in line with the conservative approach used to generate solar radiation-based prediction methods for daylight provision. Nevertheless, the method gives the user the best design solution (i.e., *WWR* when using design workflow 1), whose building performance is close to the combined fulfillment.
- **In terms of thermal comfort** (Fig. 15 (c) and (d)): In average, 89.7% of the prediction are correct (Design-*WWR*≤max*WWR*). Although wrong predictions are up to 67.1% (D1T0), the mean relative deviations are below 6.7% (Fig. 15 (c)) whereas the maximum relative deviation does not exceed 12.3%. As for daylight provision, the

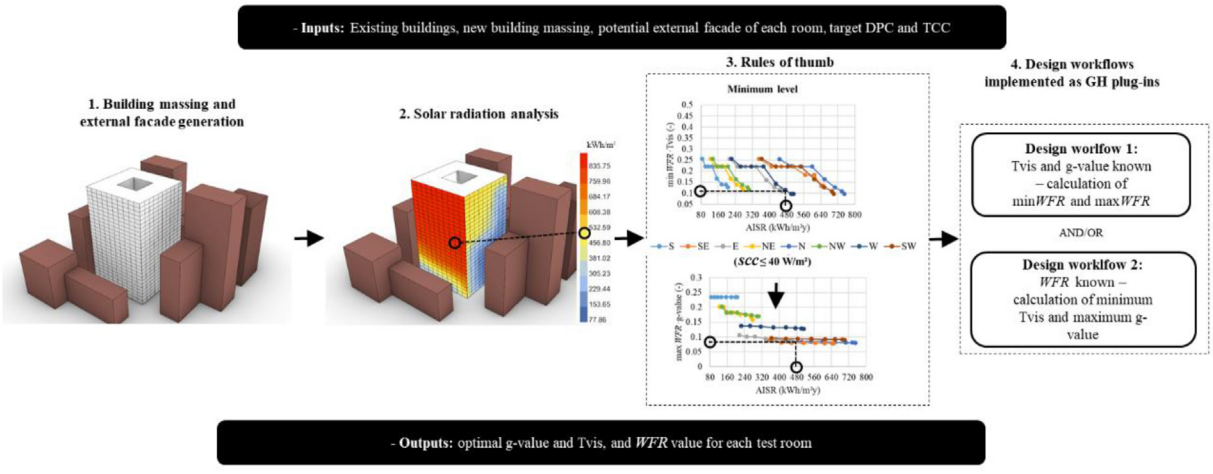

Fig. 13 Design workflows based on solar radiation-based prediction methods to achieve different level of recommendations of daylight provision (according to the EN 17037:2018) and thermal comfort.

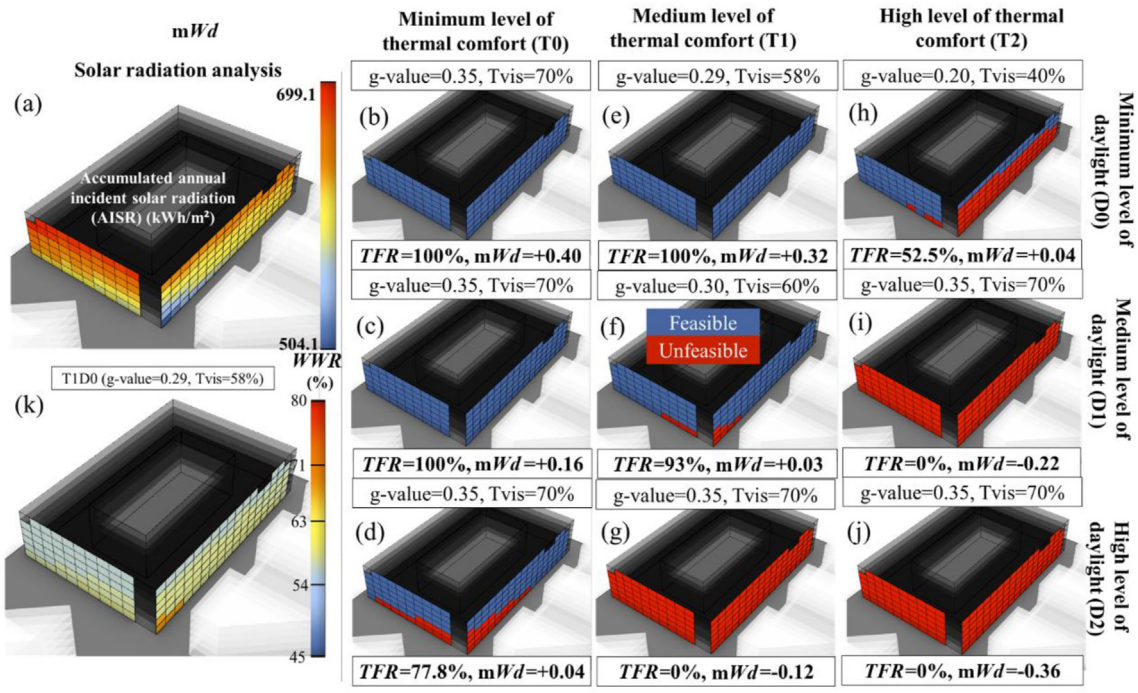

Fig. 14 Solar radiation analysis (a) required by the solar radiation-based prediction methods implemented as an open-source GH plug-in "HealthyFacadeGenerator" and optimal facade solutions to fulfill different combined requirements (b—j) between thermal comfort and daylight provision. (k) predicted optimal *WWR* values.

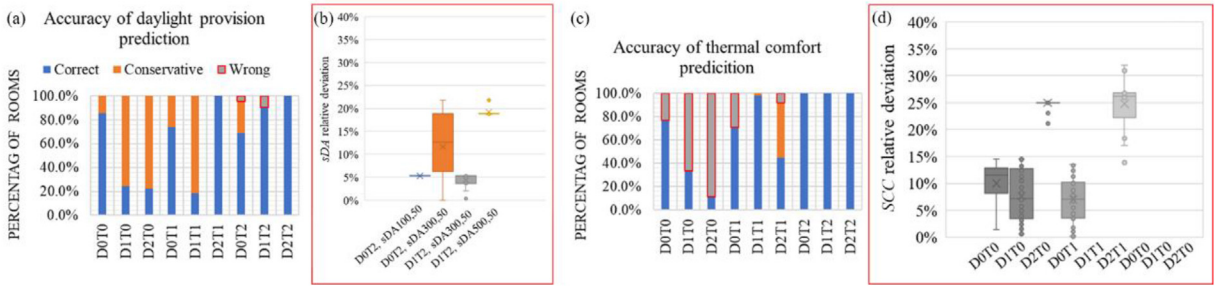

Fig. 15 Accuracy analysis of the optimization case for different design criteria: (a) daylight provision, (b) *sDA* deviations analysis, (c) thermal comfort and (d) *SCC* deviations analysis. *D* = level of daylight, *T* = level of thermal comfort, 0 = minimum, 1 = medium, 2 = high, min = minimum, and m*rd* = *sDA* mean relative deviation.

method gives the user the best design solution, whose building performance is closer to the combined fulfillment. In this case study, the prediction of the daylight provision class is less accurate and more conservative than the thermal comfort class. However, the magnitude of the relative deviations can be acceptable during the early design stages, when the number of design options is too large and the computation time is more critical than the accuracy of the performance calculations.

Regarding computation time, the use of the proposed solar radiation-based prediction methods implemented in the tool is totally justified: apart from the iterative process to select an initial design solution which could be based on experience or simulations, the time savings during early design stages for each design criterion (combination between desired daylight and thermal class) is at least 99.9982% (1.2 ms/room vs 68.35 s/room), meaning that the window sizing could be 57,000 faster than a traditional simulation based approach.

A recent study developed a machine-learning (ML) prediction model to predict daylight and thermal comfort classes in Estonian office buildings, which could optimize through a genetic algorithm (GA) glazing properties and window size per floor in a SE-oriented facade (Sepúlveda et al., 2023). The computation time required by the ML approach was more than 23 s/room, much higher than the method proposed in this research. Although the accuracy of the ML predictive method was not assessed, the possibility the *TFR* was 100% due to the floor-by-floor approach of the optimization method. In terms of purely daylight and thermal comfort classes' predictions, ML-prediction method and the proposed method based on rules of thumb could be quite similar except for medium and high

daylight provision levels (Fig. 12). Finally, the available tools and required software could make the use of these methods more or less attractive for designers, on one hand; the ML-GA method requires the use of python and grasshopper independently. On the other hand, the design workflows proposed were implemented as compact Grasshopper components for Rhinoceros, that might be easier to use by designers in practice.

4. Conclusions

There is a need to understand correlation between obstruction angle and incident solar radiation/daylight provision/cooling capacity for different facade orientations to balance daylight and thermal comfort in office buildings, especially in cold climates where there is a poor daylight availability during the cold season and high thermal mass constructions. In order to fill this research gap, the main aim of this investigation is to develop easy-to use solar radiation-based prediction methods for the design of office buildings facades (i.e., decisions: room size, *WFR*, Tvis, g-value) located in urban canyons to balance daylight provision according to the EN 17037:2018 and thermal comfort. Firstly, the scientific novelty of this investigation lays on the correlation study between the mentioned design variables and building performances (*sDA* and *SCC*). Secondly, the development of solar radiation-based prediction methods can help architects and designers to work more efficiently during early design stages and to obtain more performative solutions in much shorter time. The findings of this investigation are as follows:

- The proposal of easy-to-use solar radiation-based prediction methods to be used by architects and practitioners to balance thermal comfort (through *SCC*) and daylight provision (through *sDA*) during early design stages is possible. Thus, the solar radiation-based prediction methods are combined in two proposed design workflows not based on detailed daylight or thermal simulation, whose input is solar analyses from the building massing stage. The output of these workflows can be whether an optimal *WWR* or g-value/Tvis for each test room.
- The prediction accuracy of the solar radiation-based prediction methods depends on the desired daylight and thermal comfort classes. Considering a parametric model, which contains 61,440 rooms, the percentage of correct/conservative prediction are higher than 97.6%.
- By using the first design workflow, the facade optimization of 73,152 office rooms considering 9 different combinations of daylight and thermal comfort requirements was conducted. The building performance of an average of 77.4% rooms were correctly predicted. Apart from the time savings related to the iterative process to select an initial design solution which could be based on experience or simulations, the proposed design method is 57,000 times faster (1.1 ms/room) than a traditional approach based on daylight and energy simulations. Furthermore, the design method based on solar radiation-based prediction methods proposed in this investigation could suppose a game changer for architects and designers during early design stages within the Estonian context.

The proposed solar radiation-based prediction methods were developed considering concrete-based side-lit office rooms in the climatic context of Tallinn, Estonia. In addition, the conservative approach of selecting the most critical building performance values for each design variable could be further investigated. Despite the computation time efficiency, the level of prediction accuracy could vary depending on the case study. Solar radiation-based prediction methods could be improved by adding the energy efficiency during the cold season as a design criterion since it would limit the maximum *WFR* of the room study. There were only considered eight main room orientations, meaning that the accuracy of the design method for other orientations are unknown and might be explored in future research. The solar radiation-based prediction methods cannot give recommendations when the external facade of the room has an ASIR value out of a range that depends on the room orientation. The exclusive consideration of the direct and diffuse component but not the reflected solar radiation might make design recommendations from solar radiation-based prediction methods to overestimate thermal comfort levels. Thus, future research could be: to study the viability of the generation of the developed solar radiation-based prediction methods in other climatic context and type of buildings; the comparison of the proposed design workflows with other existing facade design methods in terms of accuracy and computation time; and qualitative evaluation of the proposed method by architects and designers to improve it.

Declaration of competing interest

The authors declare that they have no known competing financial interests or personal relationships that could have appeared to influence the work reported in this paper.

Acknowledgements

This research was partially supported by the Estonian Centre of Excellence in Zero Energy and Resource Efficient Smart Buildings and Districts, ZEBE (Grant No. 2014-2020.4.01.15-0016), the Estonian Ministry of Education and Research and European Regional Fund (Grant 2014-2020.4.01.20-0289) and the European Regional Development Fund and the Estonian Research Council (Grant No. PSG409). The authors would like to express gratitude to Hundipea OÜ for providing the early stage design models for the case study.

References

Ahmad, A.S., Hassan, M.Y., Abdullah, M.P., Rahman, H.A., Hussin, F., Abdullah, H., Saidur, R., 2014. A review on applications of ANN and SVM for building electrical energy consumption forecasting. Renew. Sustain. Energy Rev. https://doi.org/10.1016/j.rser.2014.01.069.

Batool, A., Rutherford, P., McGraw, P., Ledgeway, T., Altomonte, S., 2021. Window views: difference of perception

during the COVID-19 lockdown. LEUKOS - J. Illum. Eng. Soc. North Am. 17. https://doi.org/10.1080/15502724.2020.1854780.

CEN, 2019. EN 16798-1:2019 - Energy Performance of Buildings - Ventilation for Buildings - Part 1: Indoor Environmental Input Parameters for Design and Assessment of Energy Performance of Buildings Addressing Indoor Air Quality, Thermal Environment, Lighting and Aco.

Chen, K.W., Janssen, P., Schlueter, A., 2018. Multi-objective optimisation of building form, envelope and cooling system for improved building energy performance. Autom. ConStruct. 94. https://doi.org/10.1016/j.autcon.2018.07.002.

De Luca, F., Dogan, T., 2019. A novel solar envelope method based on solar ordinances for urban planning. Build. Simulat. 12, 817–834. https://doi.org/10.1007/s12273-019-0561-1.

De Luca, F., Sepúlveda, A., Varjas, T., 2022. Multi-performance optimization of static shading devices for glare, daylight, view and energy consideration. Build. Environ. 217, 109110. https://doi.org/10.1016/j.buildenv.2022.109110.

Domínguez-Muñoz, F., Anderson, B., Cejudo-López, J.M., Carrillo-Andrés, A., 2010. Uncertainty in the thermal conductivity of insulation materials. Energy Build. 42. https://doi.org/10.1016/j.enbuild.2010.07.006.

Duffy, J.F., Czeisler, C.A., 2009. Effect of light on human circadian physiology. Sleep Med. Clin. https://doi.org/10.1016/j.jsmc.2009.01.004.

Estonian Centre for Standardisation and Accreditation (Non-Profit Association), 2022. In: EVS-EN 17037:2019+A1: 2021.

Estonian Government, 2015. In: Ordinance N° 58. Methodology for calculating the energy performance of buildings. RTI, 09.06.2015, 21.

Estonian Government, 2012. Minimum requirements for energy performance. Annex 68. RT I, 24.01.2014, 3.

European Commission, 2018. In: BS EN 17037:2018: Daylight in Buildings.

European Commission, 2010. Directive 2010/31/EU of the European Parliament and of the Council of 19 May 2010 on the Energy Performance of Buildings (Recast). Official Journal of the European Union. https://doi.org/10.3000/17252555.L_2010.153.eng.

Fakhari, M., Fayaz, R., Asadi, S., 2021. Lighting preferences in office spaces concerning the indoor thermal environment. Front. Archit. Res. 10, 639–651. https://doi.org/10.1016/j.foar.2021.03.003.

Fanger, P.O., Christensen, N.K., 1986. Perception of draught in ventilated spaces. Ergonomics 29. https://doi.org/10.1080/00140138608968261.

Hens, H.S.L.C., 2009. Thermal comfort in office buildings: two case studies commented. Build. Environ. 44. https://doi.org/10.1016/j.buildenv.2008.07.020.

Huang, L., Fan, C., Zhai, Z., John), 2021. A graphical multi-objective performance evaluation method with architect-friendly mode. Front. Archit. Res. 10, 420–431. https://doi.org/10.1016/j.foar.2020.12.004.

Illuminating Engineering Society, The Daylight Metric Committee, 2013. LM-83-12 Approved Metric: IES Spatial Daylight Autonomy (*sDA*) and Annual Sunlight Exposure (ASE). Illuminating Engineering Society of North America (IESNA).

Kähkönen, E., 1991. Draught, radiant temperature asymmetry and air temperature — a comparison between measured and estimated thermal parameters. Indoor Air 1. https://doi.org/10.1111/j.1600-0668.1991.00008.x.

Karl-Villem, V., Eist, E., Jarek, K., 2022. Stratification and draught measurements of ceiling panels, underfloor cooling and fan-assisted radiators. In: CLIMA 2022 Conference. https://doi.org/10.34641/clima.2022.170.

Kiil, M., Mikola, A., Thalfeldt, M., Kurnitski, J., 2019. Thermal comfort and draught assessment in a modern open office building in Tallinn. In: E3S Web of Conferences. https://doi.org/10.1051/e3sconf/201911102013.

Kiil, M., Simson, R., Thalfeldt, M., Kurnitski, J., 2020. A comparative study on cooling period thermal comfort assessment in modern open office landscape in Estonia. Atmosphere (Basel) 11. https://doi.org/10.3390/atmos11020127.

Knoop, M., Stefani, O., Bueno, B., Matusiak, B., Hobday, R., Wirz-Justice, A., Martiny, K., Kantermann, T., Aarts, M.P.J., Zemmouri, N., Appelt, S., Norton, B., 2019. Daylight: what makes the difference? Light. Respir. Technol. https://doi.org/10.1177/1477153519869758.

Konis, K., Gamas, A., Kensek, K., 2016. Passive performance and building form: an optimization framework for early-stage design support. Sol. Energy 125. https://doi.org/10.1016/j.solener.2015.12.020.

Kurnitski, J., Saari, A., Kalamees, T., Vuolle, M., Niemelä, J., Tark, T., 2013. Cost optimal and nearly zero energy performance requirements for buildings in Estonia. Est. J. Eng. 19. https://doi.org/10.3176/eng.2013.3.02.

Lee, E.S., Matusiak, B., Geisler-Moroder, D., Selkowitz, S., Heschong, L., 2022. Advocating for view and daylight in buildings: next steps. Energy Build. 265, 112079. https://doi.org/10.1016/j.enbuild.2022.112079.

Li, D.H.W., Lam, J.C., Wong, S.L., 2005. Daylighting and its effects on peak load determination. Energy 30. https://doi.org/10.1016/j.energy.2004.09.009.

Li, L., Qu, M., Peng, S., 2016. Performance evaluation of building integrated solar thermal shading system: building energy consumption and daylight provision. Energy Build. 113. https://doi.org/10.1016/j.enbuild.2015.12.040.

Lockley, S.W., 2009. Circadian rhythms: influence of light in humans. In: Encyclopedia of Neuroscience. https://doi.org/10.1016/B978-008045046-9.01619-3.

Naji, S., Aye, L., Noguchi, M., 2021. Multi-objective optimisations of envelope components for a prefabricated house in six climate zones. Appl. Energy 282. https://doi.org/10.1016/j.apenergy.2020.116012.

Osterhaus, W.K.E., 2005. Discomfort glare assessment and prevention for daylight applications in office environments. In: Solar Energy. https://doi.org/10.1016/j.solener.2004.11.011.

Peel, M.C., Finlayson, B.L., McMahon, T.A., 2007. Updated world map of the Köppen-Geiger climate classification. Hydrol. Earth Syst. Sci. 11. https://doi.org/10.5194/hess-11-1633-2007.

Pilechiha, P., Mahdavinejad, M., Pour Rahimian, F., Carnemolla, P., Seyedzadeh, S., 2020. Multi-objective optimisation framework for designing office windows: quality of view, daylight and energy efficiency. Appl. Energy 261. https://doi.org/10.1016/j.apenergy.2019.114356.

Riigi, Teataja, 2020. Minimum Building Energy Efficiency Requirements.

Samuels, R., 1990. Solar efficient architecture and quality of life: the role of daylight and sunlight in ecological and psychological well-being. In: Proceedings of the 1 st World Renewable Energy Congress "Energy and the Environment", vol. 4, pp. 2653–2659.

Sepúlveda, A., 2022. A Novel Workflow for Early Design Stages to Ensure Daylight and Summer Thermal Comfort in Buildings. Tallinn University of Technology.

Sepúlveda, A., De luca, F., 2020. A multi-objective optimization workflow based on solar access and solar radiation for the design of building envelopes in cold climates. In: Symposium on Simulation for Architecture and Urban Design At. TU Wien, Vienna (Online).

Sepúlveda, A., De Luca, F., 2022. A novel multi-criteria method for building massing based on energy performance and solar access the mixed solar envelope (MSE) method. In: Co-Creating the Future — ECAADe 40, pp. 649–658.

Sepúlveda, A., De Luca, F., Kurnitski, J., 2022a. Daylight and overheating prediction formulas for building design in a cold

climate. J. Build. Eng. 45. https://doi.org/10.1016/j.jobe.2021.103532.

Sepúlveda, A., De Luca, F., Thalfeldt, M., Kurnitski, J., 2020. Analyzing the fulfillment of daylight and overheating requirements in residential and office buildings in Estonia. Build. Environ. 180. https://doi.org/10.1016/j.buildenv.2020.107036.

Sepúlveda, A., De Luca, F., Varjas, T., Kurnitski, J., 2022b. Assessing the applicability of the European standard EN 17037: 2018 for office spaces in a cold climate. Build. Environ. 225, 360–1323. https://doi.org/10.1016/j.buildenv.2022.109602.

Sepúlveda, A., Eslamirad, N., Seyed Salehi, S.S., Thalfeldt, M., De Luca, F., 2023. Machine learning-based optimization design workflow based on obstruction angles for building facades. In: Conference: 9th ECAADe Regional International Symposium (RIS2023), p. 10.

Seyed Salehi, S.S., Ferrantelli, A., Aljas, H.K., Kurnitski, J., Thalfeldt, M., 2021. Impact of internal heat gain profiles on the design cooling capacity of landscaped offices. In: E3S Web of Conferences. https://doi.org/10.1051/e3sconf/202124607003.

Seyed Salehi, S.S., Kurnitski, J., Võsa, K.-V., Thalfeldt, M., 2022. Temperature calibration and Annual performance of cooling for ceiling panels. In: 2022: CLIMA 2022 the 14th REHVA HVAC World Congress. https://doi.org/10.34641/clima.2022.344.

Sheikh, W.T., Asghar, Q., 2019. Adaptive biomimetic facades: enhancing energy efficiency of highly glazed buildings. Front. Archit. Res. 8, 319–331. https://doi.org/10.1016/j.foar.2019.06.001.

Shen, H., Tzempelikos, A., 2012. Daylighting and energy analysis of private offices with automated interior roller shades. Sol. Energy 86. https://doi.org/10.1016/j.solener.2011.11.016.

Shishegar, N., Boubekri, M., 2017. Quantifying electrical energy savings in offices through installing daylight responsive control systems in hot climates. Energy Build. 153. https://doi.org/10.1016/j.enbuild.2017.07.078.

Simson, R., 2019. Overheating Prevention and Daylight in Buildings without Mechanical Cooling. Tallinn University of Technology. https://doi.org/10.23658/taltech.54/2019.

Subramaniam, S., 2017. Daylighting Simulations with Radiance Using Matrix-Based Methods.

Thalfeldt, M., 2016. Total Economy of Energy-Efficient Office Building Facades in a Cold Climate Energy and Economic Analysis of the Facade of Energy-Efficient Office Buildings in Cold Climates.

Thalfeldt, M., Pikas, E., Kurnitski, J., Voll, H., 2017. Window model and 5 year price data sensitivity to cost-effective façade solutions for office buildings in Estonia. Energy. https://doi.org/10.1016/j.energy.2017.06.160.

Thalfeldt, M., Pikas, E., Kurnitski, J., Voll, H., 2013. Facade design principles for nearly zero energy buildings in a cold climate. Energy Build. https://doi.org/10.1016/j.enbuild.2013.08.027.

Vanhoutteghem, L., Skarning, G.C.J., Hviid, C.A., Svendsen, S., 2015. Impact of façade window design on energy, daylighting and thermal comfort in nearly zero-energy houses. Energy Build. https://doi.org/10.1016/j.enbuild.2015.05.018.

Virta, M., Butler, D., Gräslund, J., Hogeling, J., Kristiansen, E.L., Reinikainen, M., Svensson, G., 2007. Chilled Beam Application Guidebook.

Wei, Y., Zhang, X., Shi, Y., Xia, L., Pan, S., Wu, J., Han, M., Zhao, X., 2018. A review of data-driven approaches for prediction and classification of building energy consumption. Renew. Sustain. Energy Rev. https://doi.org/10.1016/j.rser.2017.09.108.

Zehnder Baltics OÜ, 2018. Zehnder Carboline.